Proceedings of ICES03
2003 Spring Technical Conference of the ASME Internal Combustion Engine Division
Salzburg, Austria, May 11-14, 2003

ICES2003-638

Numerical Simulation of Heat and Fluid Flow Behavior in a Pipe Flow with Sinusoidal Boundary Condition

M. H. Shojaee Fard[1] **A. R. Noorpoor[2]**

Mechanical Engineering Department
Iran University of science & Technology (IUST)

Abstract - *In this investigation a two-dimensional airflow and heat transfer with sinusoidal boundary condition analysis was conducted. Both laminar and turbulent sinusoidal pipe flows were investigated numerically for Re_{max}=2000, 10000, 20000 and 60000. The results are compared with experimental results of previous investigators[2], [5]. Comparing non-dimensional velocity amplitudes also checks predictions of the flow regime on present sinusoidal flow conditions. A high Reynolds number RNG $k-\varepsilon$ turbulence model was used for turbulent flows. An available code, which is basis on finite volume and can solve Nervier-stokes equations on the structured grids, is used. After discrete equations on the control volume, physical properties flux on the control volume by means of first-order upwind difference scheme is calculated. Then, to solve algebraic equations the SIMPLE method is used. Computational results are presented and discussed for velocity, pressure drop, wall shear, temperature, heat flux, and convection coefficient.*

Keywords - *sinusoidal, laminar, turbulence, numerical solution, time dependent.*

Nomenclature:

ρ: density	T: period of oscillation
ν: viscosity	u: velocity component
L: length of pipe	x: distance
P: pressure	ε: turbulent kinetic energy dissipation
Dp: pressure drop	k: turbulent kinetic energy
R: radius of pipe	τ: shear stress
r: radial distance	ω: angular frequency of oscillation
Re_{max}: maximum reynolds number	Va: $\omega R^2/\nu$

1.Prof. of Mech. Eng.
2. Ph. D. Student

1. Introduction

Harmonic turbulent problems of internal flow have been studied by many researchers experimentally as well as computationally [1]. The effect of imposed harmonic pulsation on the time-averaged properties has been previously investigated [2]. Ramaprian and Tu. found that for sufficiently high frequencies, the time-averaged flow variables, e.g., velocity, wall shear stresses, and power loss due to friction, were affected by the imposed unsteadiness [3]. They also concluded that, from their computations, a quasi-steady turbulence model can not adequately describe unsteady flow conditions, at least for high frequencies. Ohmi et al. performed extensive pulsating flow experiments to determine transition criteria via non- dimensional parameters on the basis of velocity measurements [4], [5]. Sergeev et al. investigated sinusoidal turbulent flow in pipes and rectangular ducts experimentally for various Reynoldes numbers and frequencies [6]. Many useful turbulent - flow data have been generated through their work. Rodi et al. found that the turbulent energy production becomes exceedingly high in the decelerating phase, but the turbulence is reduced to a very low level at the end of the decelerating phase and in the accelerating stage of reversal flow [7]. In this article, turbulent sinusoidal pipe flow with heat transfer has been analyzed by solving time-averaged continuity, momentum and energy equations using the RNG $k-\varepsilon$ turbulence model. A CFD computer code, based finite volume method has been used to handle unsteady inlet condition. Performance evaluation of this RNG $k-\varepsilon$ model for the present sinusoidal flow conditions will be discussed.

2. Numerical Solution

2.1 Governing equations

The time-averaged equations of continuity, momentum and energy for an unsteady Newtonian fluid with constant fluid properties can be written as follows in cylindrical form [2].

Continuity equation:

$$\frac{\partial \rho}{\partial t} + \frac{\partial}{\partial x_i}(\rho u_i) = 0 \tag{1}$$

Momentum equation:

$$\frac{\partial}{\partial t}(\rho u_i) + \frac{\partial}{\partial x_j}(\rho u_i u_j) = -\frac{\partial p}{\partial x_i} + \frac{\partial \tau_{ij}}{\partial x_j} + \rho g_i + F_i \tag{2}$$

$$\tau_{ij} = \left[\mu \left(\frac{\partial u_i}{\partial x_j} + \frac{\partial u_j}{\partial x_i} \right) \right] - \frac{2}{3} \mu \frac{\partial u_l}{\partial x_l} \delta_{ij} \tag{3}$$

where μ is the molecular viscosity and the second term on the right hand side is the effect of volume dilation.

Energy equation:

$$\frac{\partial}{\partial t}(\rho h)+\frac{\partial}{\partial x_i}(\rho u_i h)=\frac{\partial}{\partial x_i}(k+k_t)\frac{\partial T}{\partial x_i}+\frac{DP}{Dt}+\tau_{ik}\frac{\partial u_i}{\partial x_k} \tag{4}$$

$$k_t=\frac{\mu_t}{pr_t} \tag{5}$$

The transport equations for k and ε in the RNG κ-ε model are:

$$\frac{\partial k}{\partial t}+u_i\frac{\partial k}{\partial x_i}=\nu_t S^2-\varepsilon+\frac{\partial}{\partial x_i}\alpha\nu_t\frac{\partial k}{\partial x_i} \tag{6}$$

and

$$\frac{\partial \varepsilon}{\partial t}+u_i\frac{\partial \varepsilon}{\partial x_i}=C_{1\varepsilon}\frac{\varepsilon}{k}\nu_t S^2-C_{2\varepsilon}\frac{\varepsilon^2}{k}-R+\frac{\partial}{\partial x_i}\alpha\nu_t\frac{\partial \varepsilon}{\partial x_i} \tag{7}$$

α is prandtl number

$$\nu_t=C_\mu\frac{k^2}{\varepsilon} \tag{8}$$

$$C_\mu=0.0845; C_{1\varepsilon}=1042; C_{2\varepsilon}=1.68; \alpha=1.39$$

$$\eta=S\frac{k}{\varepsilon}; \eta_0\approx 4.38; S^2=2S_{ij}S_{ij}$$

$$R=\frac{C_\mu\eta^3(1-\frac{\eta}{\eta_0})\varepsilon^2}{(1+\beta\eta^3)\times k}$$

The standard wall function method is used to specify wall boundary conditions.
It should be observed that for the laminar flow regime, the flow undergoes flow reversal (near the wall), i.e., separation, during a small portion of the cycle. However, for the turbulent flow regimes, no such separation has been observed experimentally [4]. Accordingly, it appeared very plausible to use the classical wall functions for such a sinusoidal flow.
The convection fluxes in the model transport equations are discrete with the first - order upwind difference scheme.

2.2 Boundary and Initial Conditions

The flow geometry is a circular pipe, with diameter of 60 mm and length of 5,000 mm. A schematic diagram of the experimental arrangement is shown in Figure1. It consists of a piston-cylinder and a test section. At middle section, the flow can be considered fully developed. The inflow is taken to be uniform over the cross section and time dependent according to the relation.

t=0 $\Rightarrow$ u=0

x=0 $\Rightarrow u_{m,in}=|u_m|\sin\omega t$

$$T_{wall} = 1000^{\circ}K$$
$$T_{inlet} = 950^{\circ}K \tag{9}$$

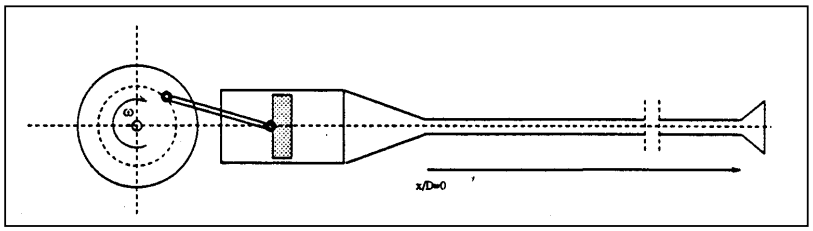

Fig.1. Schematic of the flow system

3. Flow computation and results

Four cases have been studied, Re = 2000, 10000, 20000 and 60000. In the axial and radial directions, respectively 500×30 grid nodes were used. A grid independence test has been carried-out by doubling the grid nodes. For each case, 200 time steps were used in one cycle and the results were collected after four consecutive cycles.

An computational fluid dynamics (CFD) code, which is basis on finite volume based finite difference and can solve Nervier-stokes equations on the structured grids, is used. After discrete equations on the control volume, physical properties flux on the control volume by means of first-order upwind difference scheme is calculated. Then, to solve algebraic equations the SIMPLE algorithm is used. To considering turbulence behavior of flow a high Reynolds number RNG $k-\varepsilon$ turbulence model was used. Results of numerical solution are shown in middle section of pipe.

4. Calculation in the laminar regime

Figure2 show the instantaneous velocity versus $\omega t/(\pi/6)$ at different radial locations for case1. The plots in those figures are made for the axial location at the middle of the pipe. The plots show the increase in the velocity amplitude as the distance from the wall increases. Profiles of the velocity amplitude normalized by the centerline value versus the normalized radial distance for case1 shown in Figure5.

5. Calculation in the turbulent regime

Calculations were also made for sinusoidal flows in the turbulent regime.

For turbulent computations, the RNG $k-\varepsilon$ turbulence model has been employed with standard values of the model constants.

Inlet turbulent kinetic energy k_{in} was obtained assuming isotropic turbulence [5].

$$k_{in} = \frac{3}{2}(TI \times u_{m,in})^2 \tag{10}$$

Where TI is turbulent intensity at the inlet, which is assumed to be 1 percent. Also, the turbulence length scale at the inlet l_{in} was approximated by the following equation:

$$l_{in} = \frac{k_{in}^{3/2}}{\varepsilon_{in}} \tag{11}$$

Equation 11 holds under local equilibrium conditions and for a logarithmic velocity law [5]. In this equation, the turbulent dissipation rate ε_{in} was estimated from equation 7:

$$\varepsilon_{in} = c_\mu \rho \frac{k_{in}^2}{\mu_{t,in}} \tag{12}$$

The following assumption for turbulent viscosity was used:

$$\mu_{t,in} = \sqrt{\mathrm{Re}_{max}}\, c_\mu \mu \tag{13}$$

Then Equation 12, after substituting Equation 13, becomes

$$\varepsilon_{in} = \frac{1}{\sqrt{\mathrm{Re}_{max}}} \frac{k_{in}^2}{\nu} \tag{14}$$

The turbulence length scale was estimated to about 20 percent of the pipe diameter. Computational result for case2 is shown in Figure4 in the same order as in the laminar case.

6. Critical Reynolds number

Hino et al. (1976) summarized the critical Reynolds number from several experimental and theoretical results. From their work, two critical Reynolds numbers were found for the sinusoidal pipe flow. Experimental critical Reynolds numbers are found for Re_δ based on the Stokes-layer thickness $\delta = (2\nu/\omega)^{\frac{1}{2}}$ and the cross-sectional mean velocity amplitude $|u_m|$.

$$\frac{\mathrm{Re}_{max,c}}{\sqrt{Va}} = \sqrt{2}\frac{|u_m|\delta}{\nu} = \sqrt{2}\,\mathrm{Re}_{\delta,c} \tag{15}$$

As mentioned earlier, Ohmi derived another expression for critical Reynolds number using, instead of laminar sinusoidal flow theory, the following steady turbulent correlation together with the turbulence generation region assumption mentioned previously:

$$\left.\begin{aligned} \tau_\omega &= \lambda \rho |u_m|^2 / 8 \\ \lambda &= 0.3164 / \mathrm{Re}_{max}^{1/4} \end{aligned}\right\} \tag{16}$$

They obtained the following expression Reynolds number:

$$\mathrm{Re}_{max,c} = (211\sqrt{Va})^{8/7} \tag{17}$$

7.Results and Conclusions

From Fig.3 and table1, it can be seen that ,case1 is in the laminar regime which has good agreement with experimental results and cases 2, 3 and 4 the flow fall in to the turbulent regime. Fig.3 shows *Va* versus $\mathrm{Re}_{\max}$ for the four experimental cases [2] in compare with curve result from equation 17. This confirm the Table1. Fig.2a shows laminar axial velocity profiles versus crank angle during a cycle for different radius. It shows that with increase radius $u/|u_{cl}|$ is decreased. It can be seen from Fig.2b that direction of the velocity vectors for laminar flow are changing from wall to center. This is due to periodic boundary condition. While in Fig.4 for turbulent flow at the same time and same place the velocity vectors are in one direction. Sometimes in the pipe, the direction of velocity vectors are totally changed. Fig.5 shows the comparison of experimental [2] and numerical results. Figs. 6-14 pressure drop, wall shear stress per length of pipe and mean velocity at middle section of the pipe for different Re numbers are compared with the experimental results [5]. Except Pressure drop for Re=60000 (Fig. 12), the others have very good agreement. Figs. 15, 16 and 17 are temperature, heat flux and convection coefficient at center of pipe half-length against time, respectively. It can be seen that with equilibrium of temperature the heat flux reducing to zero, and convection coefficient changes slowly.

Finally, several criteria for defining the critical Reynolds number for sinusoidal flow have been reviewed and compared according to the present numerical results. Therefore, Sinusoidal flow in a laminar flow regime can be simulated numerically with relatively high accuracy, and the RNG $k-\varepsilon$ turbulence model can predict the sinusoidal flows with good accuracy for Reynolds less than 60000. Comparing Figs. 6, 9 and 12 show that RNG $k-\varepsilon$ turbulence model could not predict the pressure and wall shear stress for high Reynolds flows, but it can predict velocity with very good accuracy.

Table -1

case	$\mathrm{Re}_{\max}$	*Va*	$\mathrm{Re}_{\max}/(Va)^{1/2}$	Experiment [2]	Regime
1	2000	80	215	217	Laminar
2	10000	172	710	410	Turbulent
3	20000	272	1171	982	Turbulent
4	60000	417	1860	1450	Turbulent

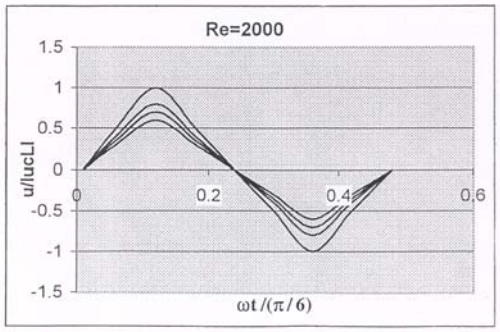

Fig.2-a. laminar axial velocity profiles versus crank angle during a cycle (were : r/R=0 , 0.25 , 0.50 , 0.80 from top)

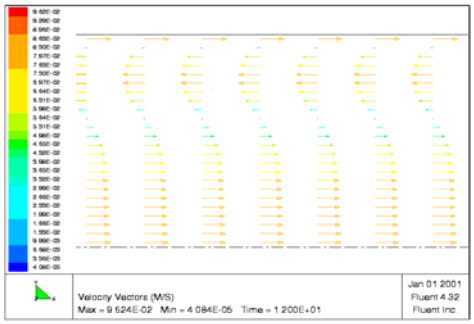

Fig.2-b. laminar velocity vectors (t=0.9sec)

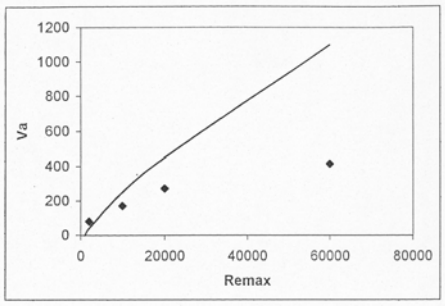

Fig.3. velocity amplitude profile at t=3sec:(• :experimental data [2])

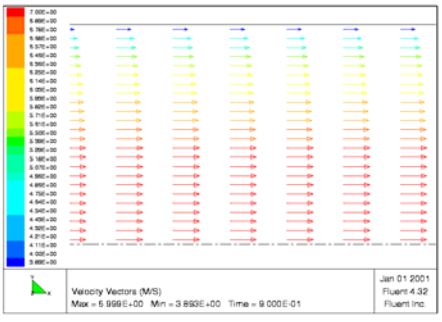

Fig.4. turbulent velocity vectors (case2, t=0.9sec)

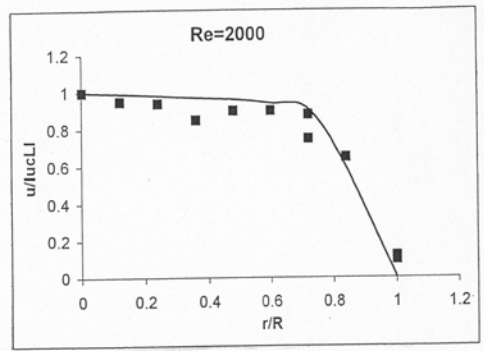

Fig.5. (• : experimental data [2])

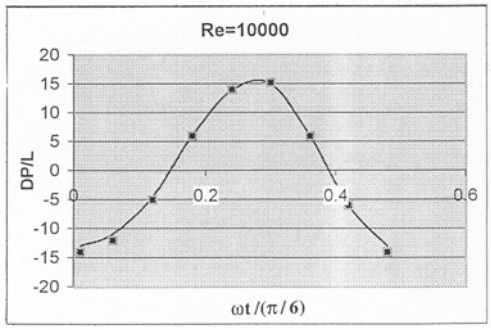

Fig.6. pressure drop per length of pipe (case2) (• : experimental data [5])

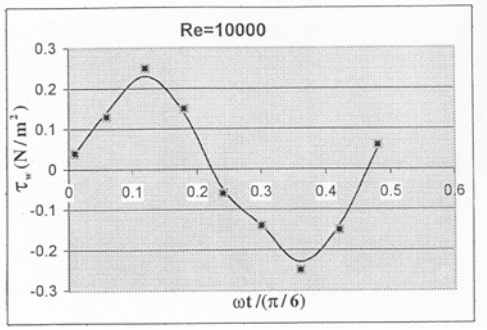

Fig.7. wall shear stress per length of pipe (case2) (• : experimental data [5])

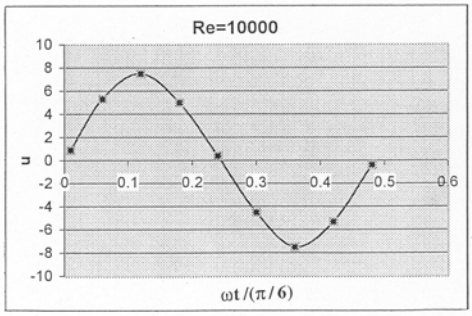

Fig.8. mean velocity at middle section of pipe (case2) (• : experimental data [5])

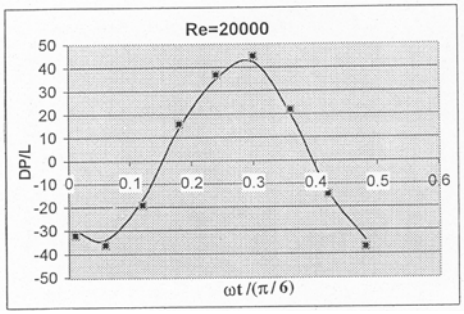

Fig.9. pressure drop per length of pipe (case3) (● : experimental data [5])

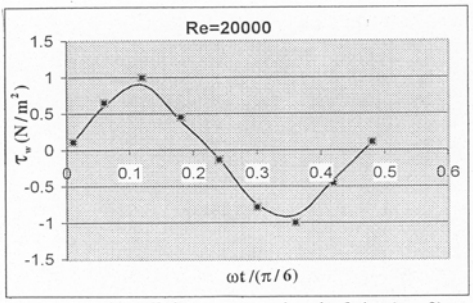

Fig.10. wall shear stress per length of pipe (case3) (● : experimental data [5])

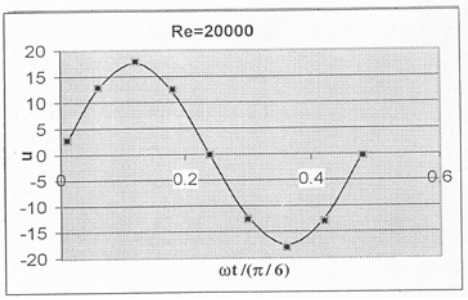

Fig.11. mean velocity at middle section of pipe (case3) (● : experimental data [5])

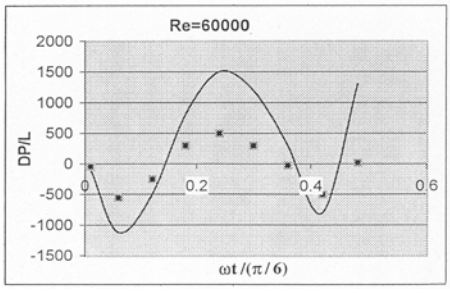

Fig.12. pressure drop per length of pipe (case4) (● : experimental data [5])

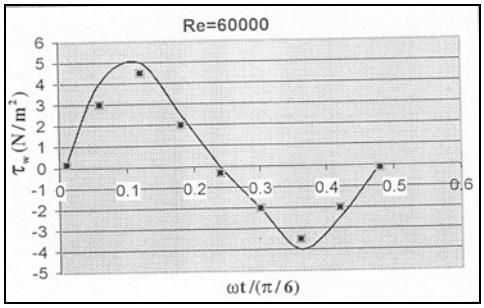

Fig.13. wall shear stress per length of pipe (case4) (● : experimental data [5])

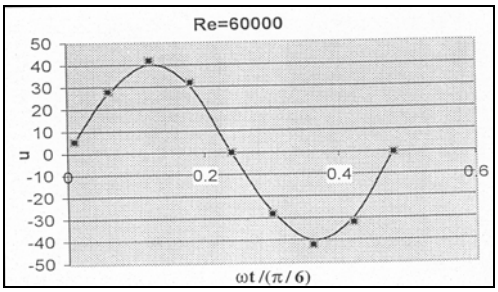

Fig.14. mean velocity at middle section of pipe (case4) (● : experimental data [5])

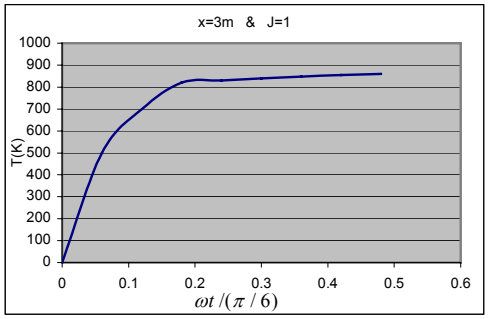

Fig.15. Temperature distribution at middle section and centerline of pipe (case4)

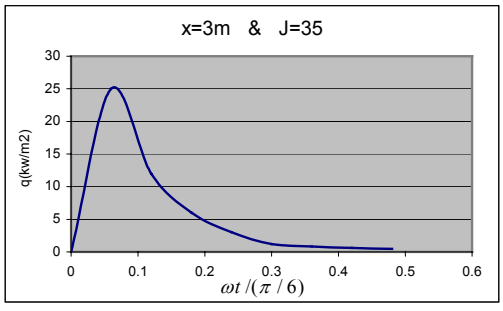

Fig.16. Heat flux distribution at middle section and centerline of pipe (case4)

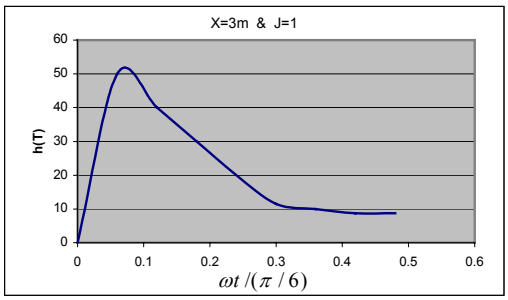

Fig.17. Convection coefficient distribution at middle section and centerline of pipe (case4)

Acknowledgment

The authors wish to thank the anonymous reviewers for providing insightful comments.

References

[1]. Launder B.E. and Spalding D.B., 1974, The numerical computation of turbulent flows, Computer Methods Appl. Mech. Eng., 3, 269 - 289.

[2]. Ohmi M. and Iguchi M., 1982, Critical Reynolds number in an oscillating pipe flow, Bull. JSME, 25(200), 165 - 172.

[3]. Ramaprian B. R. and Tu S.W., 1983, Fully developed periodic turbulent pipe flow, Part 2, The detailed structure of flow. J. Fluid Mech., 137, 59-81.

[4]. Ohmi M., Iguchi M. and Urahata I., 1982a, Transition to turbulence in a pulsation pipe flow, Bull. JSME, 25(200), 182 - 189.

[5]. Ohmi M., Iguchi M. and Urahata I., 1982b, Flow patterns and frictional losses in an oscillating pipe flow, Bull. JSME, 25(202), 536 - 543.

[6]. Sergeev S. I., 1966, Fluid oscillations in pipes at moderate Reynolds numbers, Fluid Dynam., 1,21-22.

[7]. Rodi W., 1980, Turbulence models and their application in Hydraulics a state of the art review, Int. Assoc. Hydraulic Res., Delft, 115.

[8]. Peric M., Ruger M. and Scheuerer G., 1989, A finite volume multi-grid method for calculating turbulent flows, Proc. 7th Symp. on Turbulent Shear Flows, Paper 7-3, Stanford University, 7.3.1-7.3.6.